molecules

MDPI

Article

A Novel Fluorescent Probe for Determination of pH and Viscosity Based on a Highly Water-Soluble 1,8-Naphthalimide Rotor

Ventsislav V. Bakov [1], Nikolai I. Georgiev [1,*] and Vladimir B. Bojinov [1,2,*]

[1] Department of Organic Synthesis, University of Chemical Technology and Metallurgy, 8 Kliment Ohridsky Str., 1756 Sofia, Bulgaria
[2] Bulgarian Academy of Sciences, 1040 Sofia, Bulgaria
* Correspondence: nikigeorgiev@uctm.edu (N.I.G.); vlbojin@uctm.edu (V.B.B.); Tel.: +359-2-8163207 (N.I.G.); +359-2-8163206 (V.B.B.)

Abstract: A novel highly water-soluble 1,8-naphthalimide with pH and viscosity-sensing fluorescence was synthesized and investigated. The synthesized compound was designed as a molecular device in which a molecular rotor and molecular "off-on" switcher were integrated. In order to obtain a TICT driven molecular motion at C-4 position of the 1,8-naphthalimide fluorophore, a 4-methylpiperazinyl fragment was introduced. The molecular motion was confirmed after photophysical investigation in solvents with different viscosity; furthermore, the fluorescence-sensing properties of the examined compound were investigated in 100% aqueous medium and it was found that it could be used as an efficient fluorescent probe for pH. Due to the non-emissive deexcitation nature of the TICT fluorophore, the novel system showed low yellow–green emission, which represented "power-on"/"rotor-on" state. The protonation of the methylpiperazine amine destabilized the TICT process, which was accompanied by fluorescence enhancement indicating a "power-on"/"rotor-off" state of the system. The results obtained clearly illustrated the great potential of the synthesized compound to serve as pH- and viscosity-sensing material in aqueous solution.

Keywords: 1,8-naphthalimide; twisted intramolecular charge transfer (TICT); fluorescence; pH; viscosity

Citation: Bakov, V.V.; Georgiev, N.I.; Bojinov, V.B. A Novel Fluorescent Probe for Determination of pH and Viscosity Based on a Highly Water-Soluble 1,8-Naphthalimide Rotor. *Molecules* **2022**, *27*, 7556. https://doi.org/10.3390/molecules27217556

Academic Editors: Guido Viscardi and Andrea Fin

Received: 8 October 2022
Accepted: 2 November 2022
Published: 4 November 2022

1. Introduction

Due to the rapid progress in the fields of chemosensing materials and nanotechnology, the design and synthesis of molecular switches have received considerable attention in recent years [1–4]. A wide range of different architectures applied as various molecular devices [5–10], object-coding [11], chemical-sensing [12,13], data-storage [14,15], drug-delivery [16,17], and drug-activation [18,19] systems have been obtained. Among them, major attention has been paid to fluorescence sensors and probes due to the several advantages, such as cheap equipment, high sensitivity, immediate response, and great spectral resolution. In addition, they have a small, safe, and indestructible signaling nature which allows their practical application even in real-time imagining of living organisms [20–24].

The lack of water-solubility is the main disadvantage of fluorescent probes, which seriously restricts their usage. Currently, chemical analysis in water solutions, in the absence of organic solvents, was preferable due to the use of environmentally friendly media with lower cytotoxicity and higher biocompatibility, which is, especially, suitable for bioimagining purposes; therefore, the design and synthesis of highly water-soluble fluorescent probes has increasingly attracted considerable interest [25–29]. This encouraged us to prepare and investigate the chemosensing properties of a novel fluorescent probe with high solubility in 100% water media. The compound presented in Scheme 1 under study is a TICT (twisted intramolecular charge transfer) molecular rotor with fluorescence-sensing

properties focusing on pH and viscosity. The rapid analysis of pH and viscosity plays a critical role in large areas of industrial production, food processing, and environmental monitoring [30–37]; also, the abnormal values of intracellular pH and viscosity could be associated with several diseases, such as atherosclerosis, Alzheimer's disease, diabetes, and cancer [38–42]; hence, the synthesis of fluorescent probes for both pH and viscosity currently could be of significant importance. In order to simultaneously achieve pH- and viscosity-switchable fluorescence, the novel probe was based on a TICT molecular rotor platform. It is well known that deexcitation from the TICT state is non-radiative or shows batochromically shifted (lower energy) emission than normal fluorescence which was successfully utilized for the imaging of viscosity in biological objects [43,44]; furthermore, the TICT process is microenvironmentally dependable and can be easily switched at different pHs [45].

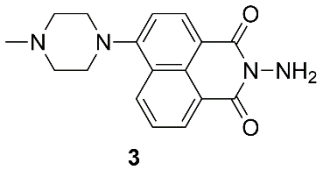

3

Scheme 1. Chemical structure of 1,8-naphthalimide-based probe **3**.

2. Results and Discussion

2.1. Design and Synthesis

The compound under study (**3**) was designed as a fluorescence-sensing TICT rotor based on a 4-piperazinyl-1,8-naphthalimide architecture. The 1,8-naphthalimide fluorophore was chosen as a fluorogenic unit due to its bright fluorescence, large stokes shift, and high photo and chemical stabilities [46–48]. The *N*-methylpiperazine fragment was bound to the C-4 position of the 1,8-naphthalimide unit in probe **3** to achieve TICT molecular motion. It is well known that the presence of dialkylamines such as *N*-methylbuthylamine, morpholine, piperidine, and piperazine at C-4 position resulted in a TICT process in the fluorophore-excited state and they could be used as fluorescent probes for viscosity [49–52]; additionally, the protonation of *N*-methylpiperazine amine destabilized the irradiative TICT process, thus preventing rotation and allowing significant emission increase which was widely utilized in the pH-probe design [9,53,54]. Furthermore, the presence of different amines at *N*-position of the 1,8-naphthaimides resulted in a significant increase in their water solubility [25,55,56]. This was our motive to introduce a primary amino group in position *N* of the novel probe.

The examined compound **3** was easily synthesized from available sources in two steps according Scheme 2.

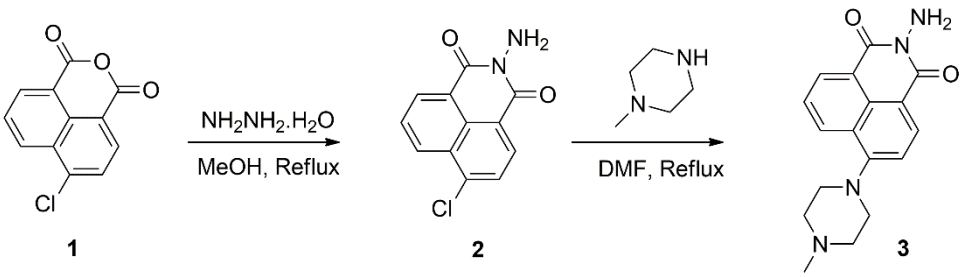

1 **2** **3**

Scheme 2. Synthesis of probe **3**.

First, hydrazine monohydrate was condensed with 4-cloro-1,8-naphthalic anhydride using equimolar amounts in methanol solution under reflux; then, the chlorine in intermediate **2** was, subsequently, substituted with *N*-methylpiperazine in boiling DMF solution for 5 h to afford final probe **3** as yellow crystals.

2.2. Chemosensing Properties of Probe 3

2.2.1. pH-Sensing Properties

The synthesized compound **3** was designed as a fluorescent probe with high water solubility. This was the reason to study its photophysical properties in 100% water solution (in the absence of organic solvents). It was found that in acid and neutral media probe **3** showed an absorption band in a range of 300–500 nm with maximum at 394 nm that was slightly red, shifting under alkaline conditions to 406 nm (Figure 1). Such behavior is common for 4-amino-1,8-naphthalimides containing aminoalkylamines at position C-4 and easy could be rationalized according to the internal charge transfer (ICT) occurring in the excited state of these chromophoric systems. The light absorption of 1,8-naphthaimides results in a charge transfer from the C-4 electron-donating group to the electron-accepting carbonyls, which efficiency determines the basic photophysical properties of the molecule [57–59]. For a difference, in neutral and acid media the methylpiperazine nitrogen is in its protonated form and exerts a weak charge repulsion on the 4-amino moiety directly attached to the ICT cromophoric system in probe **3**. This decreased the ICT efficiency and slightly shifted the observed absorption band towards higher energy wavelengths.

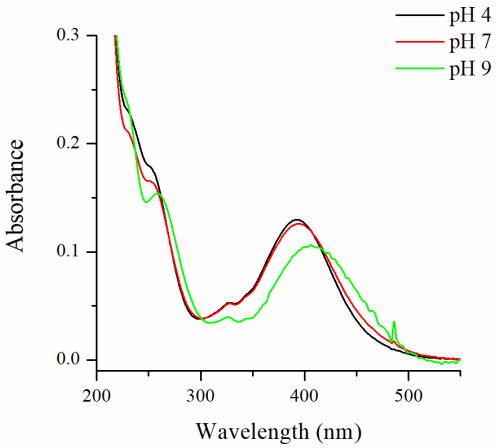

Figure 1. Absorption spectra of probe **3** in aqueous solution at different pHs.

In alkaline media probe **3** showed a very low fluorescence emission in the range of 450–650 nm, with maximal value at 550 nm (Figure 2A); however, the protonation of the methylpiperazine amine after addition of hydrochloric acid gradually increased the fluorescence output of **3** and blue shifted its maximum to 530 nm. The calculated quantum yield of fluorescence was Φ_F = 0.001 at pH 12 and Φ_F = 0.14 at pH 4.

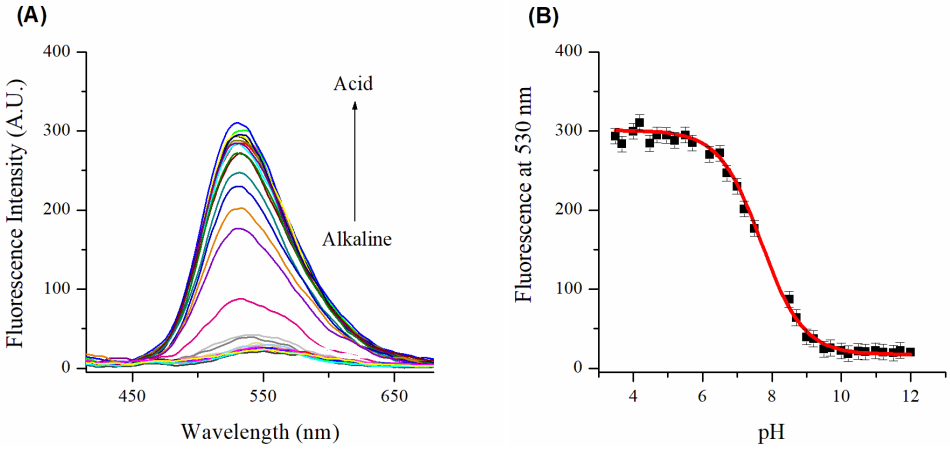

Figure 2. (**A**) Fluorescent spectra of probe **3** in 100% aqueous solution in a pH interval of 4–12 (λ_{ex} = 400 nm) and (**B**) pH titration plot of probe **3** fluorescence intensity at 530 nm.

The observed fluorescent enhancement in acid media was expectable and, in recent works, it was attributed to the fact that the ICT in 4-methylpiperzinyl-1,8-naphthalimides undergoes a twisting process (TICT) with nonradiative deexcitation nature [51]. The protonated methylpiperazine nitrogen generates a positively charged cation that leads to electrostatic destabilization of the TICT state, thus reducing its deexcitation channel. As a result, a bright fluorescence was observed. From the fluorescent changes at 530 nm as a function of pH, a well pronounced S-shaped (sigmoidal Boltzmann fit, $R^2 = 0.9977$) titration plot was observed, suggesting a simple thermodynamic equilibrium (Figure 2B).

It was found that the reversible pH-switching process appeared in pH window 6–9, giving a pK_a value of 7.69 ± 0.05 according to the Hendersen-Hasselbalch Equation (1), which matches the previous reported pK_a value of 4-methylpiperzinyl-1,8-naphthalimide derivatives [51].

$$\mathrm{pH} = \mathrm{p}K_a + \log \frac{(I_{max} - I)}{(I - I_{min})} \quad (1)$$

where I_{max} and I_{min} are the maximum and minimum fluorescence intensity, respectively, and I is the fluorescence intensity at the corresponding pH value.

Furthermore, the difference in the TICT and normal states showed that the deexcitation of **3** could be used as a molecular rotor with power indicator at molecular level giving us information about the presence or lack of motion in the TICT system. The non-emissive TICT deexcitation nature of **3** shows very low yellow-green emission, which represents the "power-on"/"rotor-on" state of the system. The protonation of the methylpiperazine amine destabilizes the TICT process, thus enhancing the fluorescence intensity of probe **3,** indicating a "power-on"/"rotor-off" state of the system (Scheme 3).

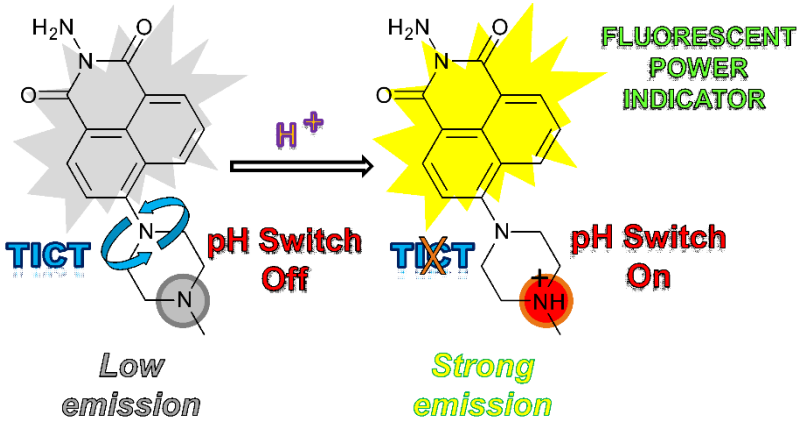

Scheme 3. Switching mechanism of probe **3** as a function of pH.

The effects of the most common cations and anions (Co^{2+}, Cu^{2+}, Fe^{3+}, Ni^{2+}, Pb^{2+}, Cd^{2+}, Zn^{2+}, Hg^{2+}, Cl^-, NO_3^-, SO_4^{2-}, HSO_4^-, CO_3^{2-}, CH_3COO^-, Br^-, NO_2^-, SO_3^{2-}, PO_4^{3-}, and F^-) on the fluorescent emission of **3** were tested as potential analytes or interferents. The study was performed in aqueous media at pH 7.2 (10 μM HEPES) and pH 8 (10 μM Tris-HCl). In both cases, the tested ions (10^{-5} mol/L and 10^{-4} mol/L) caused only a minor quenching (below 10%) of the probes' (10^{-5} mol/L) fluorescence intensity; also, it was found that the studied probe **3** could be transferred between "off" and "on" states reversibly at least nine times without changes in the fluorescence intensity in both acid and alkaline media (Figure 3). These results clearly showed that compound **3** is stable in a wide pH range and could be used as a selective and efficient platform for rapid determination of pH values in aqueous solutions.

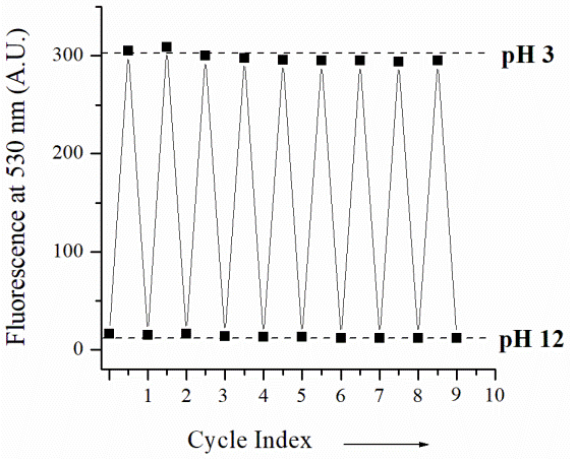

Figure 3. Cycle index of probe **3**.

2.2.2. Viscosity-Sensing Properties

The fluorescence properties of **3** were investigated in solvents with different viscosities in order to confirm the existence of TICT molecular motion in the examined compound. The higher viscosity seriously restricts the intramolecular bond rotation and prevents the TICT process. The influence of viscosity on the fluorescence spectra of **3** was defined after measurements in glycol, glycerol, and glycol/glycerol mixtures (Figure 4). As can be seen from Figure 3, the probe **3** showed viscosity-sensing fluorescence intensity increasing in a high viscous solution. A double logarithmic scale of the fluorescent intensity at 530 nm of compound **3** and solvent viscosity (Figure 4, Inset) showed a relationship with good linearity (R^2 = 0.9843) which is typical for TICT rotors [36,37].

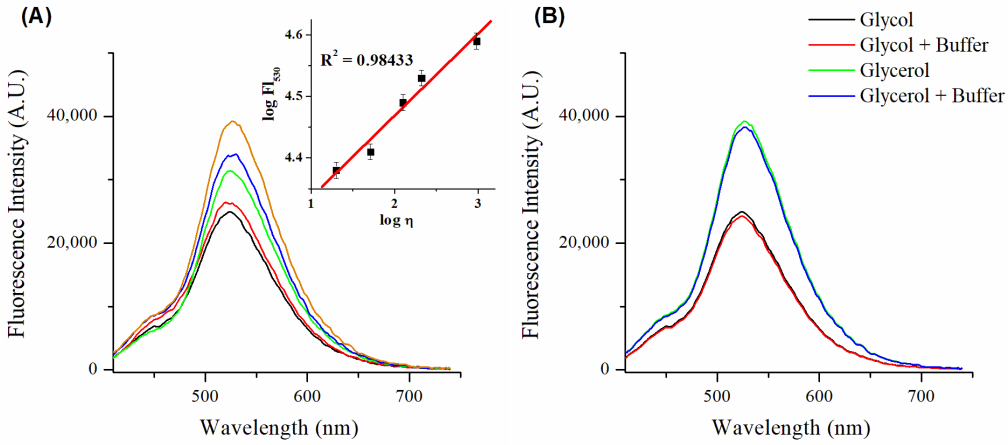

Figure 4. Normalized to the optical density fluorescent spectra (λ_{ex} = 400 nm) of probe **3** (**A**) in glycol (black line), glycol/glycerol = 3:2 *v*/*v* (red line), glycol/glycerol = 1:1 *v*/*v* (blue line), glycol/glycerol = 2:3 *v*/*v* (green line), and glycerol (orange line), and (**B**) in glycol, buffered glycol containing 10 μM Tris-HCl (pH 8), glycerol, and buffered glycerol containing Tris-HCl (pH 8).

Glycerol has lower pK_a value than glycol and the acidity of the glycerol/glycol mixture could be a major reason for the observed fluorescence changes. In order to reject this theory, the fluorescent spectra of **3** were measured in glycol, buffered glycol containing 10 μM Tris-HCl (pH 8), glycerol, and buffered glycerol containing Tris-HCl (pH 8). The results presented in Figure 4B show that the presence of buffer solution did not lead to a significant result which clearly illustrated that the changes in fluorescence intensity of **3** mainly were induced due to the different viscosity. The results suggested the existence of fluorescence quenching in **3** with the nature of the TICT deexcitation path making it a promising fluorescent probe for viscosity.

2.2.3. Molecular Logic

As a whole, the above fluorescence-sensing properties of probe **3** logically could be summarized in an OR molecular logic gate (Figure 5). In low-viscosity solution (glycol, coded in binary as 0) and in the absence of protons (HCl, coded in binary as 0), **3** showed a very low fluorescence output which was coded in binary as 0; however, in solution with high viscosity (glycerol, coded in binary as 1) and in the absence of protons (hydrochloric acid, coded in binary as 0), probe **3** fluorescence was higher (coded in binary as 1) due to the hindered TICT quenching effect. In the presence of protons (HCl 10^{-6} mol/L, coded in binary as 1), due to the destabilization of the TICT excited state, probe **3** showed viscosity independent of high fluorescence output (coded in binary as 1). In other words, the novel probe shows high fluorescence at high viscosity or high acidity, or both high viscosity and high acidity. This behavior correlated very well with an OR logic gate. Obviously, the novel probe **3** could be used as OR molecular logic gate, using viscosity and protons as inputs and fluorescence emission as output.

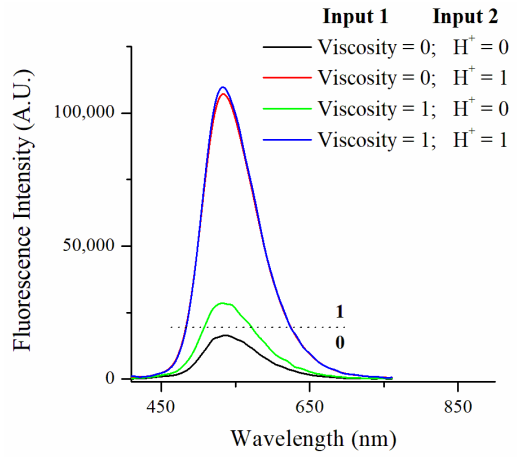

Figure 5. OR molecular logic gate based on probe **3** using different viscosity and protons as inputs.

In addition, it should be pointed out that in the presence of protons in glycerol the observed emission was higher than in glycerol without acid. This could have been the result of a possible photoinduced electron transfer (PET) from tertiary piperazine amine to the excited fluorophore, which quenched the fluorescence in glycerol. The protonation of the tertiary amine disallowed the PET quenching, thus, the addition of acid in glycerol solution resulted in a brighter fluorescence [51].

3. Materials and Methods

3.1. Materials

The starting reagents 4-chloro-1,8-naphthalic anhydride, hydrazine monohydrate, and *N*-methylpiperazine were used as commercial products (Sigma-Aldrich Co., St. Louis, MO, USA and Fisher Scientific, Waltham, MA, USA) without purification. All solvents used in the synthetic procedures and in the photophysical investigation (Sigma-Aldrich Co., St. Louis, MO, USA and Fisher Scientific, Waltham, MA, USA) were pure or of spectroscopy grade. As sources of metal cations, $Zn(NO_3)_2$, $Cu(NO_3)_2$, $Ni(NO_3)_2$, $Co(NO_3)_2$, $Pb(NO_3)_2$, $Fe(NO_3)_3$, $Hg(NO_3)_2$, and $Cd(NO_3)_2$ were used (all Aldrich salts at p.a. grade). KCl, $NaNO_3$, Na_2SO_4, $NaHSO_4$, Na_2CO_3, CH_3COONa, KBr, $NaNO_2$, Na_2SO_3, K_3PO_4, and NaF were the sources of anions (all salts at p.a. grade).

3.2. Methods

FT-IR spectra were recorded on a Thermo Scientific Nicolet iS20 FTIR spectrometer (Thermo Fisher Scientific, Waltham, MA, USA). The ^{1}H NMR analysis was performed on a Bruker AV-600 spectrometer (BRUKER AVANCE II+ 600 MHz, Bruker, Billerica, MA, USA) with operating frequency at 600 MHz. Electrospray ionization mass spectra (ESI-MS) were

obtained on a Bruker MicrOTOF-Q system (Compass, Bruker Billerica, MA, USA). The TLC monitoring was performed on silica gel, ALUGRAM®SIL G/UV254, 40 × 80 mm, 0.2 mm silica gel 60. A Hewlett-Packard 8452A spectrophotometer (Agilent Technologies, Inc., Santa Clara, CA, USA) was used for the UV-Vis absorption measurements. The photophysical study was performed at room temperature (25.0 °C) in 1 × 1 cm quartz cuvettes. The fluorescence spectra were recorded using a Scinco FS-2 spectrofluorimeter (Scinco, Seoul, Korea). The quantum yields of fluorescence (Φ_F) were calculated relatively to Coumarin 6 (Φ_F = 0.78 in ethanol) [60]. Very small volumes of hydrochloric acid and sodium hydroxide were used to adjust the pH which was monitored by HANNA® Instruments HI-2211 benchtop pH meter (HANNA Instruments, Woonsocket, RI, USA). The influence of metal cations and anions on the fluorescence emission was studied by adding portions of ion stock solution to a 10 mL of the fluorophore solution. The addition was limited to 100 µL so that dilution remained insignificant. The ions were added gradually up to 10 equivalents (10^{-4} mol/L) to a fluorophore solution (10^{-5} mol/L). The effect of ions was studied at constant pH in the presence of 10 µM HEPES (pH 7.2) or 10 µM Tris-HCl (pH 8) buffer solutions. The viscosity measurements were performed in binary mixtures of ethylene glycol/glycerol using an Ubbelohde capillary viscometer (Sigma-Aldrich Co., St. Louis, MO, USA).

3.3. Synthetic Procedures

3.3.1. Synthesis *N*-Amino-4-chloro-1,8-naphthalimide **2**

A hydrazine monohydrate (0.2 mL, 400 mmol) was added to a solution of 4-chloro-1,8-naphthalic anhydride **1** (1 g, 400 mmol) in 20 mL of methanol. The resulting mixture was heated under reflux for 3 h. After cooling, the precipitate was filtered off, washed with methanol, and dried to produce pale yellow crystals of *N*-amino-4-chloro-1,8-naphthalimide **2** (0.77 g, 78%). FT-IR (KBr) cm^{-1}: 3314 and 3236 (ν NH_2); 1702 (ν^{as} N-C=O); 1652(ν^{s} N-C=O).

3.3.2. Synthesis of Probe **3**

To a solution of *N*-amino-4-chloro-1,8-naphthalimide **2** (0.5 g, 2 mmol) in 5 mL of DMF, 0.4 mL of methylpiperazine (8 mmol) was added; then, the resulting solution was heated under reflux for 5 h. The precipitated solid after cooling was filtered off and dried. The final 1,8-naphthalimide **3** was obtained as yellow crystals (0.62 g, 99%) after azeotropic distillation of the solvent (DMF) in the presence of *n*-heptane. FT-IR (KBr) cm^{-1}: 3331 and 3335 (νNH_2); 1693 (ν^{as}N-C=O); and 1633 (ν^{s}N-C=O). ^{1}H NMR ($CHCl_3$-*d*, 600.13 MHz) ppm: 8.53 (dd, 1H, *J* = 7.3 Hz, *J* = 1.1 Hz, naphthalimide H-5); 8.46 (d, 1H, *J* = 8.1 Hz, naphthalimide H-2); 8.36 (dd, 1H, *J* = 8.4 Hz, *J* = 1.1 Hz, naphthalimide H-7); 7.63 (dd, 1H, *J* = 8.4 Hz, *J* = 7.3 Hz, naphthalimide H-6); 7.15 (d, 1H, *J* = 8.1 Hz, naphthalimide H-3); 5.44 (br.s, 2H, NH_2); 3.26 (m, 4H, 2 × NCH_2); 2.69 (m, 4H, 2 × CH_3NCH_2); and 2.38 (s, 3H, CH_3). Elemental analysis: Calculated for $C_{17}H_{18}N_4O_2$ (MW 310.35) C 65.79, H 5.85, N 18.05%; Found C 66.01, H 5.79, N 17.88%. Positive-ion ESI-MS at *m*/*z*: 311.0145 $[M + H]^+$.

4. Conclusions

In conclusion, a novel highly water-soluble 1,8-naphthalimide with pH- and viscosity-sensing fluorescence was designed using TICT molecular motion. The photophysical investigation of the synthesized compound was performed in an aqueous solution and in solvents with different viscosities. The results obtained revealed its potential to serve as a fluorescent probe for rapid detection of pH and viscosity, which was attributed to the destabilization of the TICT excited state in acid media and hindered rotation at high viscosity. The results presented here could be seen as a contribution to the development of the applied sensory chemistry using environmentally friendly aqueous media.

Author Contributions: Conceptualization, V.B.B. and N.I.G.; methodology, N.I.G.; formal analysis, N.I.G. and V.V.B.; investigation, V.V.B. (synthesis and photochemistry); writing—original draft preparation, N.I.G.; writing—review and editing, V.B.B.; supervision, V.B.B.; and funding acquisition, V.B.B. All authors have read and agreed to the published version of the manuscript.

Funding: This research was funded by the National Science Fund of Bulgaria (grant number KP-06-H39/3).

Institutional Review Board Statement: Not applicable.

Informed Consent Statement: Not applicable.

Data Availability Statement: The authors declare that the data supporting the findings of this study are available within the article.

Conflicts of Interest: The authors declare no conflict of interest.

Sample Availability: Samples of the compounds are available from the authors.

References

1. Steinegger, A.; Wolfbeis, O.S.; Borisov, S.M. Optical Sensing and Imaging of pH Values: Spectroscopies, Materials, and Applications. *Chem. Rev.* **2020**, *120*, 12357–12489. [CrossRef] [PubMed]
2. De Silva, A.P. Crossing the divide: Experiences of taking fluorescent PET (photoinduced electron transfer) sensing/switching systems from solution to solid. *Dye. Pigment.* **2022**, *204*, 110453. [CrossRef]
3. Hamilton, G.; Sahoo, S.; Kamila, S.; Singh, N.; Kaur, N.; Hyland, B.; Callan, J. Optical probes for the detection of protons, and alkali and alkaline earth metal cations. *Chem. Soc. Rev.* **2015**, *44*, 4415–4432. [CrossRef] [PubMed]
4. De, S.; Das, G. Exploring the Aggregation and Light-Harvesting Aptitude of Naphthalimide-Based Amphiphile and Non-amphiphile AIEgen. *Langmuir* **2022**, *38*, 6158–6163. [CrossRef]
5. Zhang, Q.; Rao, S.-J.; Xie, T.; Li, X.; Xu, T.-Y.; Li, D.-W.; Qu, D.-H.; Long, Y.-T.; Tian, H. Muscle-like Artificial Molecular Actuators for Nanoparticles. *Chem* **2018**, *4*, 2670–2684. [CrossRef]
6. Shirai, Y.; Morin, J.-F.; Sasaki, T.; Guerrero, J.; Tour, J. Recent progress on nanovehicles. *Chem. Soc. Rev.* **2006**, *35*, 1043–1055. [CrossRef]
7. Chen, W.; Guo, C.; He, Q.; Chi, X.; Lynch, V.; Zhang, Z.; Su, J.; Tian, H.; Sessler, J. Molecular Cursor Caliper: A Fluorescent Sensor for Dicarboxylate Dianions. *J. Am. Chem. Soc.* **2019**, *141*, 14798–14806. [CrossRef]
8. Slavcheva, S.; Mendoza, J.; Stanimirov, S.; Petkov, I.; Basílio, N.; Pina, F.; Petrov, V. On the multistate of 2′-hydroxyflavylium-flavanone system. Illustrating the concept of a timer with reset at the molecular level. *Dye. Pigment.* **2018**, *158*, 465–473. [CrossRef]
9. Georgiev, N.; Marinova, N.; Bojinov, V. Design and synthesis of light-harvesting rotor based on 1,8-naphthalimide units. *J. Photochem. Photobiol. A Chem.* **2020**, *401*, 112733. [CrossRef]
10. Nakashima, K.; Georgiev, A.; Yordanov, D.; Matsushima, Y.; Hirashima, S.; Miura, T.; Antonov, L. Solvent-Triggered Long-Range Proton Transport in 7-Hydroxyquinoline Using a Sulfonamide Transporter Group. *J. Org. Chem.* **2022**, *87*, 6794–6806. [CrossRef]
11. Ling, J.; Naren, G.; Kelly, J.; Moody, T.; de Silva, A.P. Building pH sensors intopaper-based small-molecular logic systems for very simple detection of edgesof objects. *J. Am. Chem. Soc.* **2015**, *137*, 3763–3766. [CrossRef] [PubMed]
12. Xu, S.; Xing, X.; Liu, Y.; Gao, H. A hemicyanine-based fluorescence probe for selective detection of CYP2D6 in living cells and tumor-bearing mice. *Dye. Pigment.* **2022**, *198*, 109959. [CrossRef]
13. Georgiev, N.; Krasteva, P.; Bakov, V.; Bojinov, V. A Highly Water-Soluble and Solid State Emissive 1,8-Naphthalimide as a Fluorescent PET Probe for Determination of pHs, Acid/Base Vapors, and Water Content in Organic Solvents. *Molecules* **2022**, *27*, 4229. [CrossRef] [PubMed]
14. Hou, Y.; Du, J.; Hou, J.; Shi, P.; Wang, K.; Zhang, S.; Han, T.; Li, Z. Rewritable optical data storage based on mechanochromic fluorescence materials with aggregation-induced emission. *Dye. Pigment.* **2019**, *160*, 830–838. [CrossRef]
15. Cafferty, B.; Ten, A.; Fink, M.; Morey, S.; Preston, D.; Mrksich, M.; Whitesides, G. Storage of Information Using Small Organic Molecules. *ACS Cent. Sci.* **2019**, *5*, 911–916. [CrossRef]
16. Ruskowitz, E.; Comerford, M.; Badeau, B.; DeFores, C. Logical stimuli-triggered delivery of small molecules from hydrogel biomaterials. *Biomater. Sci.* **2019**, *7*, 542–546. [CrossRef]
17. Romero, M.; Mateus, P.; Matos, B.; Acuña, Á.; García-Río, L.; Arteaga, J.; Pischel, U.; Basílio, N. Binding of Flavylium Ions to Sulfonatocalix[4]arene and Implication in the Photorelease of Biologically Relevant Guests in Water. *J. Org. Chem.* **2019**, *84*, 10852–10859. [CrossRef]
18. Todorov, P.; Peneva, P.; Georgieva, S.; Tchekalarova, J.; Vitkova, V.; Antonova, K.; Georgiev, A. Synthesis, characterization and anticonvulsant activity of new azobenzene-containing UV-hemorphin-5 bio photoswitch. *Amino Acids* **2019**, *51*, 549–563. [CrossRef]
19. Turan, I.; Gunaydin, G.; Ayan, S.; Akkaya, E. Molecular demultiplexer as a terminator automaton. *Nat. Commun.* **2018**, *9*, 805. [CrossRef]

20. Georgiev, N.I.; Bryaskova, R.G.; Ismail, S.R.; Philipova, N.D.; Uzunova, V.P.; Bakov, V.V.; Tzoneva, R.D.; Bojinov, V.B. Aggregation induced emission in 1,8-naphthalimide embedded nanomicellar architecture as a platform for fluorescent ratiometric pH-probe with biomedical applications. *J. Photochem. Photobiol. A Chem.* **2021**, *418*, 113380. [CrossRef]
21. Yang, X.; Lovell, J.F.; Murthy, N.; Zhang, Y. Organic Fluorescent Probes for Diagnostics and Bio-Imaging. *Top. Med. Chem.* **2020**, *34*, 33–53.
22. Shen, R.; Qian, Y. A mitochondria-oriented fluorescent probe for ultrafast and ratiometric detection of HSO_3^- based on naphthalimide-hemicyanine. *New J. Chem.* **2019**, *43*, 7606–7612. [CrossRef]
23. Guo, F.-F.; Wu, W.-N.; Zhao, X.-L.; Wang, Y.; Fan, Y.-C.; Zhang, C.-X.; Xu, Z.-H. A deep-red lysosome-targetable fluorescent probe for detection of hypochlorous acid in pure water and its imaging application in living cells and zebrafish. *Spectrochim. Acta Part A* **2022**, *264*, 120270. [CrossRef] [PubMed]
24. Gond, S.; Yadava, P.; Chauhan, B.; Srikrishna, S.; Singh, V. Development of an 'OFF-ON-OFF' colorimetric and fluorometric pH sensor for the study of physiological pH and its bioimaging application. *J. Mol. Struct.* **2022**, *1252*, 132147. [CrossRef]
25. Johnson, A.D.; Zammit, R.; Vella, J.; Valentino, M.; Buhagiar, J.A.; Magri, D.C. Aminonaphthalimide hybrids of mitoxantrone and amonafide as anticancer and fluorescent cellular imaging agents. *Bioorg. Chem.* **2019**, *93*, 103287. [CrossRef] [PubMed]
26. Jung, J.M.; Kang, J.H.; Han, J.; Lee, H.; Lim, M.H.; Kim, K.-T.; Kim, C. A novel "off-on" type fluorescent chemosensor for detection of Zn^{2+} and its zinc complex for "on-off" fluorescent sensing of sulfide in aqueous solution, in vitro and in vivo. *Sens. Actuators B Chem.* **2018**, *267*, 58–69. [CrossRef]
27. Zhang, Y.; Zhao, Y.; Song, B.; Huang, C. Spectroscopic behavior and intracellular application of a highly sensitive UV-fluorescence double ratio probe based on water-soluble indole for detection acid pH. *Dye. Pigment.* **2021**, *188*, 109205. [CrossRef]
28. Georgiev, N.; Said, A.; Toshkova, R.; Tzoneva, R.; Bojinov, V. A novel water-soluble perylenetetracarboxylic diimide as a fluorescent pH probe: Chemosensing, biocompatibility and cell imaging. *Dye. Pigment.* **2019**, *160*, 28–36. [CrossRef]
29. Li, X.; Gao, X.; Shi, W.; Ma, H. Design strategies for water-soluble small molecular chromogenic and fluorogenic probes. *Chem. Rev.* **2014**, *114*, 590–659. [CrossRef]
30. Ozdemir, M. Two Colorimetric and Fluorescent Dual-Channel Chemosensors for the Selective Detection of pH in Aqueous Solutions. *ChemistrySelect* **2020**, *5*, 14340–14348. [CrossRef]
31. Thottiparambil, A.; Kumar, P.; Chakkumkumarath, L. Styrylcyanine-based ratiometric and tunable fluorescent pH sensors. *RSC Adv.* **2014**, *4*, 56063–56067. [CrossRef]
32. Wang, X.; Huang, D.; Niu, C.; Guo, L.; Cui, J.; Hu, L.; Zeng, G. An internal reference fluorescent pH sensor with two pH-sensitive fluorophores carrier. *Sens. Actuators B* **2016**, *234*, 593–601. [CrossRef]
33. Gotor, R.; Ashokkumar, P.; Hecht, M.; Keil, K.; Rurack, K. Optical pH sensor covering the range from pH 0-14 compatible with mobile-device readout and based on a set of rationally designed indicator dyes. *Anal. Chem.* **2017**, *89*, 8437–8444. [CrossRef] [PubMed]
34. Khan, M.; Mukherjee, K.; Shoukat, R.; Dong, H. A review on pH sensitive materials for sensors and detection methods. *Microsyst. Technol.* **2017**, *23*, 4391–4404. [CrossRef]
35. Koenig, M.; Storti, B.; Bizzarri, R.; Guldi, D.; Brancato, G.; Bottari, G. A fluorescent molecular rotor showing vapochromism, aggregation-induced emission, and environmental sensing in living cells. *Mater. Chem. C* **2016**, *4*, 3018–3027. [CrossRef]
36. Liu, T.; Liu, X.; Spring, D.; Qian, X.; Cui, J.; Xu, Z. Quantitatively Mapping Cellular Viscosity with Detailed Organelle Information via a Designed PET Fluorescent Probe. *Sci. Rep.* **2014**, *4*, 5418. [CrossRef]
37. Wu, Z.-Y.; Cui, J.-N.; Qian, X.-H.; Liu, T.-Y. A 4-aminonaphthalimide based environmentally sensitive fluorescence probe. *Chin. Chem. Lett.* **2013**, *24*, 359–361. [CrossRef]
38. Han, J.; Burgess, K. Fluorescent Indicators for Intracellular pH. *Chem. Rev.* **2010**, *110*, 2709–2728. [CrossRef]
39. Zhou, J.; Zhang, L.; Tian, Y. Micro Electrochemical pH Sensor Applicable for Real-Time Ratiometric Monitoring of pH Values in Rat Brains. *Anal. Chem.* **2016**, *88*, 2113–2118. [CrossRef]
40. Nan, M.; Niu, W.; Fan, L.; Lu, W.; Shuang, S.; Li, C.; Dong, C. Indole-based pH probe with ratiometric fluorescence behavior for intracellular imaging. *RSC Adv.* **2015**, *5*, 99739–99744. [CrossRef]
41. Song, H.; Zhang, W.; Zhang, Y.; Yin, C.; Huo, F. Viscosity activated NIR fluorescent probe for visualizing mitochondrial viscosity dynamic and fatty liver mice. *Chem. Eng. J.* **2022**, *445*, 136448. [CrossRef]
42. Wei, Y.-F.; Zhang, X.-Q.; Xu, Y.-J.; Sun, R.; Ge, J.-F. Fluorescent probes based 1,8-naphthalimide-nitrogen heterocyclic for monitoring the fluctuation of mitochondrial viscosity. *Dye. Pigment.* **2021**, *194*, 109559. [CrossRef]
43. Sasaki, S.; Drummen, G.; Konishi, G. Recent advances in twisted intramolecular charge transfer (TICT) fluorescence and related phenomena in materials chemistry. *J. Mater. Chem. C* **2016**, *4*, 2731–2743. [CrossRef]
44. Raja, S.; Sivaraman, G.; Mukherjee, A.; Duraisamy, C.; Gulyani, A. Facile Synthesis of Highly Sensitive, Red-Emitting, Fluorogenic Dye for Microviscosity and Mitochondrial Imaging in Embryonic Stem Cells. *ChemistrySelect* **2017**, *2*, 4609–4616. [CrossRef]
45. Das, M.; Brahma, M.; Krishnamoorthy, G. Controlling the photoswitching of 2-(4′-diethylamino-2′-hydroxyphenyl)-1H-imidazo-[4,5-b]pyridine by pH. *J. Photochem. Photobiol. A Chem.* **2021**, *421*, 113504. [CrossRef]
46. Rudebeck, E.; Cox, R.; Bell, T.; Acharya, R.; Feng, Z.; Gueven, N.; Ashton, T.; Pfeffer, F. Mixed alkoxy/hydroxy 1,8-naphthalimides: Expanded fluorescence colour palette and in vitro bioactivity. *Chem. Commun.* **2020**, *56*, 6866–6869. [CrossRef] [PubMed]
47. Jin, R.; Ahmad, I. Theoretical study on photophysical properties of multifunctional star-shaped molecules with 1,8-naphthalimide core for organic light-emitting diode and organic solar cell application. *Theor. Chem. Acc.* **2015**, *134*, 89. [CrossRef]

48. Saini, A.; Bhasin, A.; Singh, N.; Kaur, N. Development of a Cr(III) ion selective fluorescence probe using organic nanoparticles and its real time applicability. *New J. Chem.* **2016**, *40*, 278–284. [CrossRef]
49. Szakacs, Z.; Rousseva, S.; Bojtar, M.; Hessz, D.; Bitter, I.; Kallay, M.; Hilbers, M.; Zhang, H.; Kubinyi, M. Experimental evidence of TICT state in 4-piperidinyl-1,8-naphthalimide—A kinetic and mechanistic study. *Phys. Chem. Chem. Phys.* **2018**, *20*, 10155–10164. [CrossRef]
50. Chen, Y.; Qi, J.; Huang, J.; Zhou, X.; Niu, L.; Yan, Z.; Wang, J. A nontoxic, photostable and high signal-to-noise ratio mitochondrial probe with mitochondrial membrane potential and viscosity detectivity. *Spectrochim. Acta Part A* **2018**, *189*, 634–641. [CrossRef]
51. Lynch, S.; Rice, T.; Moody, T.; Gunaratne, H.; de Silva, A. Structural effects on the pH-dependent fluorescence of naphthalenic derivatives and consequences for sensing/switching. *Photochem. Photobiol. Sci.* **2012**, *11*, 1675–1681.
52. Chi, W.; Chen, J.; Qiao, Q.; Gao, Y.; Xu, Z.; Liu, X. Revealing the switching mechanisms of an OFF-ON-OFF fluorescent logic gate system. *Phys. Chem. Chem. Phys.* **2019**, *21*, 16798–16803. [CrossRef] [PubMed]
53. Spiteri, J.; Johnson, A.; Denisov, S.; Jonusauskas, G.; McClenaghan, N.; Magri, D. A fluorescent AND logic gate based on a ferrocene-naphthalimide-piperazine format responsive to acidity and oxidizability. *Dye. Pigment.* **2018**, *157*, 278–283. [CrossRef]
54. Pais, V.; Remón, P.; Collado, D.; Andréasson, J.; Pérez-Inestrosa, E.; Pischel, U. OFF-ON-OFF Fluorescence Switch with T-Latch Function. *Org. Lett.* **2011**, *13*, 5572–5575. [CrossRef]
55. Xie, J.; Chen, Y.; Yang, W.; Xu, D.; Zhang, K. Water soluble 1,8-naphthalimide fluorescent pH probes and their application to bioimagings. *J. Photochem. Photobiol. A Chem.* **2011**, *223*, 111–118. [CrossRef]
56. Georgiev, N.; Dimov, S.; Asiri, A.; Alamry, K.; Obaid, A.; Bojinov, V. Synthesis, selective pH-sensing activity and logic behavior of highly water-soluble 1,8-naphthalimide and dihydroimidazonaphthalimide derivatives. *J. Lumin.* **2014**, *149*, 325–332. [CrossRef]
57. Liu, J.; de Silva, A.P. Path-selective photoinduced electron transfer (PET) in a membrane-associated system studied by pH-dependent fluorescence. *Inorg. Chim. Acta* **2012**, *381*, 243–246. [CrossRef]
58. Marinova, N.; Georgiev, N.; Bojinov, V. Synthesis and photophysical properties of novel 1,8-naphthalimide lightharvesting antennae based on benzyl aryl ether architecture. *J. Lumin.* **2018**, *204*, 253–260. [CrossRef]
59. Wang, L.; Wang, G.; Shang, C.; Kang, R.; Fang, Y. Naphthalimide-Based Fluorophore for Soft Anionic Interface Monitoring. *ACS Appl. Mater. Interfaces* **2017**, *9*, 35419–35426. [CrossRef]
60. Reynolds, G.; Drexhage, K. New coumarin dyes with rigidized structure for flashlamp-pumped dye lasers. *Opt. Commun.* **1975**, *13*, 222–225. [CrossRef]